Auto-Calibration and Control Strategy Determination for a Variable-Speed Heat Pump Water Heater Using Optimization

ABSTRACT

This paper introduces applications of the GenOpt® optimizer coupled with a vapor compression system model for auto-calibration and control strategy determination towards the development of a variable-speed ground-source heat pump water heating unit. The GenOpt® optimizer can be linked with any simulation program using input and output text files. It effectively facilitates optimization runs. Using our GenOpt® wrapper program, we can flexibly define objectives for optimizations, targets, and constraints. Those functionalities enable running extensive optimization cases for model calibration, configuration design and control strategy determination. In addition, we describe a methodology to improve prediction accuracy using functional calibration curves. Using the calibrated model, we investigated control strategies of the ground-source heat pump water heater, considering multiple control objectives, covering the entire operation range.

INTRODUCTION

Hardware-based vapor compression system models are used widely in product design, performance prediction, and control strategy determination. Simulation-driven design significantly shortens product development cycles and reduces cost. However, simulation models can only approximate the real world performance; they never provide the exact system performance due to many unknowns. An un-calibrated model can be misleading, and the model calibration is a critical step in the design process. A usual simulation-driven design procedure may include: using a simulation model to select concepts (design); building a bread board unit for obtaining data, which is used to calibrate the simulation model (calibration); using the calibrated simulation model to optimize the component and system configurations, as well as deciding the control strategy (optimization); building an improved configuration to verify the performance goals (verification); and using the verified system model to develop an optimal control strategy. An optimal control strategy usually coordinates operations of the components inside the system to achieve expected performance. The optimization step usually considers trade-off between the product performance and cost.

At the calibration step, common practices involve using constant Performance Adjustment Factors (PAF) to scale or offset the model predictions, for matching the measured performance at one design point. Rossi (1995) developed a complete tuning approach for a single-stage vapor compression system model that uses measurements at one design point for the refrigerant inlet and outlet states of each component and air-side boundary conditions. For the condenser or evaporator, inlet conditions and measured refrigerant mass flow rate are inputs, and then the air-side and refrigerant-side heat transfer coefficients are tuned with one multiplier to give an outlet enthalpy that matches the value associated with the measured outlet pressure and temperature.

Recent advancements in variable-speed products, i.e. variable-speed compressors and fans, bring in new challenges in model calibrations, since the model inaccuracies change with mass flow rate and other driving factors like source and sink temperatures. Correlating the PAFs with the driving factors will improve the model accuracy in a larger range, which is called functional calibration. In addition, variable speed systems have more variables to adjust. In order to achieve optimum performance, a control strategy for matching the adjustable variables has to be carefully investigated. An accurate model over an extensive operation range is a key for product optimization and control strategy determination.

A functional calibration approach adjusts the PAFs to match the model predictions to the measurements at multiple testing points, and then curve-fits the PAFs as a function of significant driving parameters. Since for variable-speed equipment the data points can be numerous, manual calibration process becomes tedious and error-prone. It is necessary to use auto-calibration tools and batch- run functionality.

Engineering optimization is a powerful design tool. It provides a systematic way of finding a global optimum design. In this paper we are using optimization in its rigorous definition (Radermacher and Abdelaziz 2008) to assist in both simulation model calibration and control strategy determination. This work depends on GenOpt®, which is an optimization program for the minimization of a cost function evaluated by an external simulation program (Wetter 2009). GenOpt® has 6 built-in optimization algorithms and 2 parametric study algorithms. Available optimization algorithms are: Generalized Pattern Search algorithm (Hooke-Jeeves and Coordinate Search algorithm), Particle Swarm Optimization algorithm, hybrid global optimization algorithm (Particle Swarm Optimization for the global optimization, and Hooke-Jeeves for the local optimization, Discrete Armijo Gradient algorithm, Nelder and Mead's Simplex algorithm, and Golden Section and Fibonacci algorithms for one-dimensional minimization. Parametric studies algorithms in GenOpt® can be done either using a mesh generator to evaluate the function on all points that belong to a mesh with equidistant or logarithmic spacing between the mesh points or parametric search where only one independent variable is varied at a time. More details about these algorithms are discussed by Wetter (2009). GenOpt® allows the coupling of any simulation program with its built-in optimization algorithms. This coupling is achieved by properly setting the optimization problem using the configuration file. GenOpt® communicates with simulation programs using text files. It automatically generates input files for the simulation program based on predefined templates that include keywords describing the problem variables. The configuration file includes all the information regarding the simulation program: how it can be started and how to retrieve the current value of the cost function. As such, GenOpt® can be used with any simulation program that can read its input from text files and write the cost function value plus any possible error messages to a text file. In the case of constrained optimization as is the case with most engineering applications, GenOpt® provides a default algorithm for box-constraints. Users can also provide their own penalty or barrier functions as part of the problem definition.

In this paper, we use a vapor compression system simulation tool to evaluate the performance of a variable-speed ground-source heat pump water heater. A software wrapper was developed to provide seamless coupling between GenOpt® and the system simulation tool. We used this wrapper for auto-calibration, configuration optimization, and control strategy determination. It should be mentioned, this paper is more about an engineering design practice rather than introducing an innovative optimization method. Our focus is to manage multiple variables in an all-variable-speed heat pump product, considering the all-variable-speed product and the related design practice are quite new. The paper will illustrate how to take in multiple test data to improve the model accuracy at extensive working conditions, rather than a usual single-point calibration; how to coordinate the operations of all the components to achieve optimum performance in the entire envelope, while avoid going beyond control constraints.

GENOPT® OPTIMIZATION WRAPPER

Engineering optimization problems involve at least one objective function that is either minimized or maximized. Examples include maximizing energy efficiency, capacity, reliability, or minimizing cost, energy consumption, materials, leaks, etc. The result is a global optimum design that satisfies all the problem constraints. Optimization problems are usually subject to equality and/or inequality constraints within a specified design space as shown in Equation (1). In Equation (1), f refers to the objective function of the optimization problem, x is a vector of d design variables, g_i represents the i^{th} inequality constraint, I is the number of inequality constraints, h_j is the j^{th} equality constraints and J is the number of equality constraints. The vectors x_k^L and x_k^U indicate the lower and the upper bounds of the variable x_k respectively.

$$\begin{aligned} &\underset{x}{\text{minimize}} \quad f(x) \\ &\text{subject to}: g_i(x) \le 0 \qquad i = 1,.....,I \\ &\qquad\qquad h_j(x) = 0 \qquad j = 1,.....,J \\ &\qquad\qquad x_k^L \le x_k \le x_k^U \quad k = 1,.....,d \end{aligned} \tag{1}$$

We developed a GenOpt® optimization wrapper as shown in Figure 1. GenOpt® automatically generates input files for the simulation program based on predefined templates that include keywords describing the problem variables. The input files should be ASCII text files. GenOpt® may not be compatible with any simulation software directly, for example, some programs use xml files as inputs. In addition, GenOpt® provides generic minimization algorithm, which doesn't work directly if we want to maximize or match against a variable. In the case of finding multiple optimization objectives, they might conflict with one another so weighting factors are needed to quantify the relative importance. Thus, we developed a wrapper program, which communicates the inputs and outputs between GenOpt® and the simulation program, and supplies the performance outputs for minimization.

As shown in Figure 1, the problem domain is defined in two parts, One part defines required inputs for the GenOpt® program (in the GenOpt command file), which selects the optimization algorithm and regulates design spaces for the iterative variables; the other part (in the wrapper template file) defines attributes and design spaces for the selected objectives. The wrapper program accepts three kinds (attributes) of objectives: optimization objectives, target objectives (equality constraints), and bound objectives (inequality constraints). An optimization objective is to maximize or minimize an output variable, a target objective intends to match the output variable to a given value, and a bound objective is to define upper and lower bounds for an output variable.

GenOpt® produces guess values for the iterative variables through a text file to the wrapper program. The wrapper program interprets the input file to provide the required inputs for the vapor compression system model, and then executes the model to get performance outputs. Then, the wrapper program provides the outputs in the form shown in Equation (2).

$$\begin{aligned} f(x) &= \sum (W_i * OptObj_i) + \sum [T_j * (TgtObj_j - Goal_j)]^2 \\ &+ \sum [P_k * (BndObj_k - Bound_k)]^2 \end{aligned} \tag{2}$$

where $f(x)$ is the integrated function to be minimized by the GenOpt® algorithm, x is a vector of the model variables to be iterated , and W_i is the weighting factor for an optimization objective. $OptObj_i$ is a variable for optimization, it will be maximized by giving a negative weighting factor, and minimized by giving a positive weighting factor. $TgtObj_j$ is a variable intended to match a given target value, and T_j is a weighting factor to be multiplied with the residual. $Goal_j$ is a given target value. $BndObj_k$ is an output variable having either upper or lower bound. $Bound_k$ is a given boundary value. P_k is a penalty factor, which is zero when the output variable is within the given bounds; on the other hand, it becomes a quite large multiplier when the output variable goes beyond the bounds.

Next, GenOpt® evaluates the result of the output function, and updates the guesses for the iterative variables. The interaction process between GenOpt® and the wrapper program is repeated until the minimum of the output function is found. For the analyses below, the optimization algorithm applied was Generalized Pattern Search algorithm (Hooke-Jeeves and Coordinate Search algorithm).

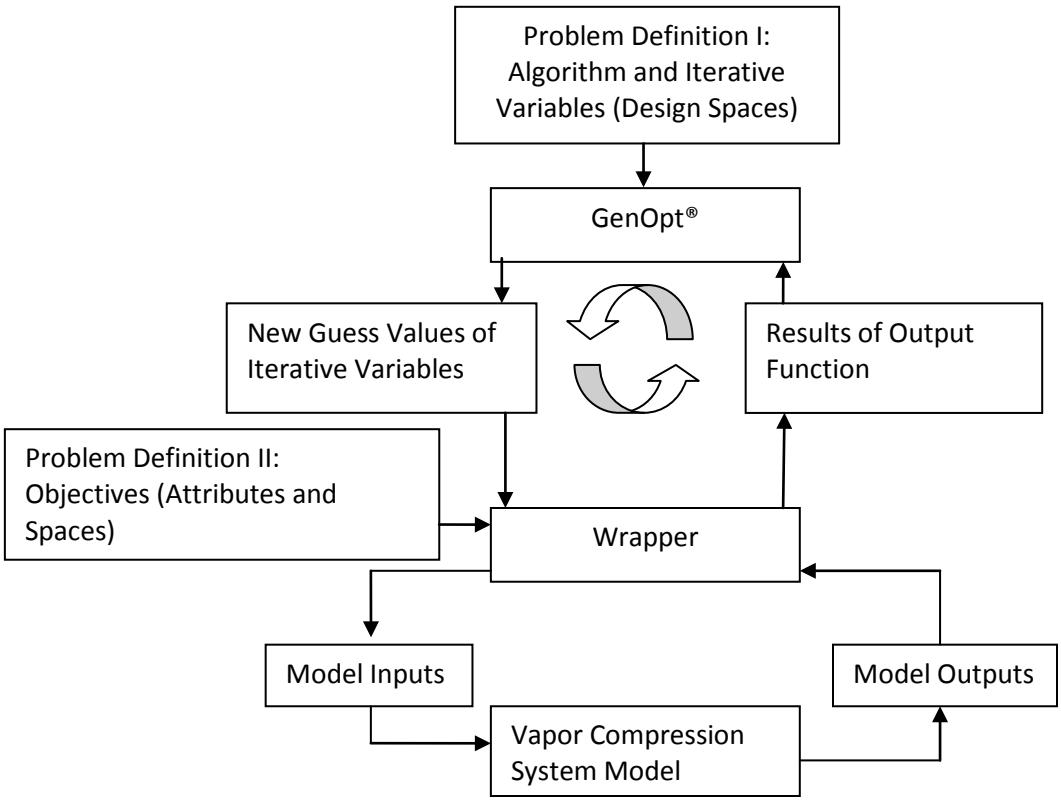

Figure 1: GenOpt® Optimization Wrapper to a Vapor Compression System Model

GROUND SOURCE HEAT PUMP WATER HEATER

We analyzed a ground source heat pump water heater as illustrated in Figure 2. It has a variable-speed rotary compressor (C), a variable-speed water heater pump (PI), a variable-speed ground pump (PO), an electronic expansion valve (EEV) to control the refrigerant flow, one double-walled tube-in-tube, refrigerant-to-water heat exchanger (HXRWI) for water heating, and one single-walled tube-in-tube, refrigerant-to-glycol heat exchanger as the source evaporator (HXRWO). The refrigerant is in the annulus of each tube-in-tube heat exchanger. The source evaporator is to be connected to a ground loop heat exchanger (GC), where glycol is the working fluid. The heated water is to be stored in a domestic hot water tank (WT).

A laboratory breadboard heat pump unit with the above components minus the variable-speed pumps was tested for forty test conditions covering an extensive operation range, with compressor speed (HZ) varied from 50 HZ to 100 HZ, water temperature entering the water heater (EHWT) varied from 21.1 °C (70°F) to 54.4 °C (130°F), and water temperature entering the source evaporator (EWT) varied from 0 °C (32°F) to 21.1 °C (70°F). Basically, the EHWT was varied at four levels, 21.1 °C (70 °F), 32.2 °C (90 °F), 43.3 °C (110 °F) and 54.4 °C (130 °F). The EWT was varied at three levels, 0 °C (32 °F), 10 °C (50 °F) and 21.1 °C (70 °F). At EWT of 0 °C (32 °F), the compressor speed was varied at 80, 90 and 100 HZ; at EWT of 10 °C (50 °F), the compressor speed was varied at 60, 70, and 80 HZ; at EWT of 21.1 °C (70 °F), the compressor speed was varied at 50, 60, 70 HZ. However, no data was available with varying water flow rates, due to laboratory testing constraints. The water heating loop and the ground loop were operated at the nominal flow rates.

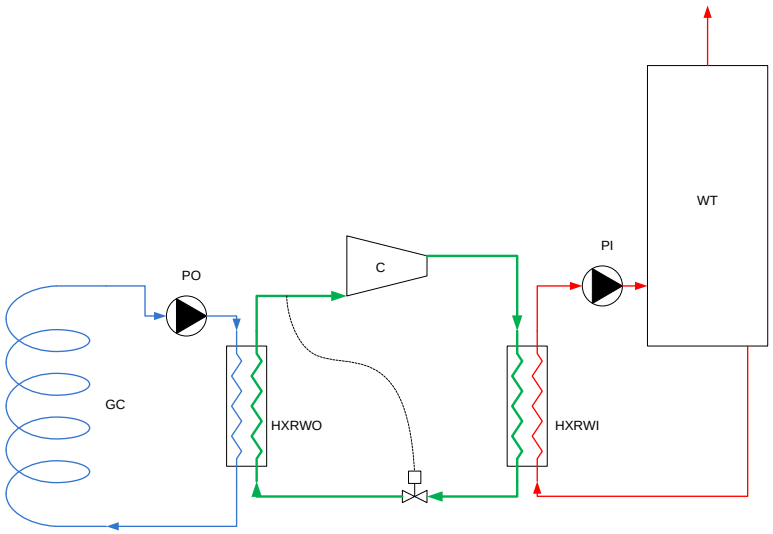

Figure 2: Water Source Heat Pump Water Heater

HEAT PUMP SIMULATION MODEL

We used the system model developed by Rice (2005) to simulate the ground source heat pump water heater. The system model uses an ARI ten-coefficient compressor map to calculate compressor mass flow rate and power consumption for a fixed compressor speed. In order to simulate a variable-speed compressor, multiple sets of map coefficients, specific to individual compressor speeds, are utilized and the model performs a linear or quadratic interpolation between speed levels. For modeling a tube-in-tube, refrigerant-to-water heat exchanger (either condenser or evaporator), it uses a phase-to-phase modeling approach; accepts tube geometries like tube length, inner volumes, groove number, angle and depth, etc.; single-phase fluid (water or glycol) can be on either side. The heat transfer correlations for the tube-in-tube model were modeled after Rousseau et al (2003). The system model also provides detailed charge calculations. We simulated variable-speed pumps in the model by utilizing curves of pump power versus flow rate for assumed system head curves for the ground and domestic hot water loops. By finding the cross points of the pump head curves and the assumed system head curves at individual pump speeds, we obtained the relationship of pump power as a function of the pump flow rate, which is according to each EWT or EHWT. At last, we fitted the pump power consumption as a 2-dimensional function, depending on both the pump flow rate and the heat exchanger entering temperature. The system simulation can be run by specifying either subcooling degree or charge inventory, along with compressor inlet superheat. These options were used in the calibration and optimization stages, respectively. The system model is able to accept functional calibration curves, i.e. PAFs as a function of significant driving parameters like compressor speed, ambient temperature, EWT, etc.

MODEL CALIBRATION

There are numerous reasons for model calibration: heat exchanger models don't necessarily capture all the geometry and manufacturing details, the compressor map is representative of the compressor model but is not specific to the test compressor, the superheat degree controlled by the electronic expansion valve might vary at different glycol entering temperatures; and due to unknown environmental conditions, accurate calculations of the compressor shell heat loss and suction line heat gain are generally not possible.

The available experimental measurements facilitated model calibration for: compressor power consumption,

compressor shell heat loss ratio to the compressor power, suction line heat gain, condenser and evaporator heat transfer and superheat and subcooling degrees. It should be mentioned that the refrigerant mass flow rate was not measured, and so we made no adjustments to the map-predicted refrigerant mass flow rate. In addition, the discharge line heat loss can be ignored, and the heat exchanger pressure drops were calibrated using a constant multiplier.

Some of the PAFs can be obtained by directly comparing the component model with the measured data, e.g. the compressor power corrections, shell heat loss ratios, suction line heat gains, and superheat degrees. Figures 3 and 4 illustrate how the compressor power adjustment coefficients (measured/map) vary with compressor speed, EWT, and EHWT. Apparently, a single adjustment coefficient can't compensate for the inaccuracies in the entire range.

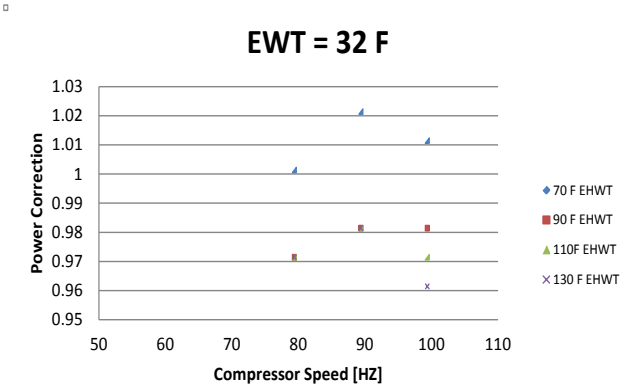

Figure 3: Compressor Power Multipliers (EWT = 0 °C, 32°F)

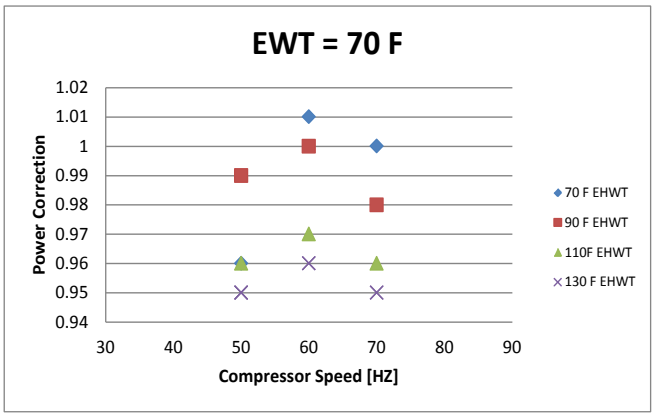

Figure 4: Compressor Power Multipliers (EWT = 21.1 °C, 70°F)

On the other hand, there exist other PAFs that depend on the components' interaction within the system. Such calibration requires an overall system performance evaluation. The calibration objective is to minimize the error between modeled and measured performance. This optimization study was performed using GenOpt® and the model wrapper discussed earlier. In this problem, we want to vary the heat transfer multipliers for the evaporator and the condenser, requiring the simulated evaporating and condensing pressures to match the measured targets. For calibrating the heat transfer, the vapor compression system model was run specifying the measured subcooling degrees. We have forty test points, each of which represents an individual problem domain. In the case, we set up a batch run to automate the point-by-point calibration process.

We only had two measured quantities, i.e. condensing saturation temperature and evaporating saturation temperature, In order to calibrate the heat transfer, it is impossible to decouple the water side heat transfer from the refrigerant side using one test point. One common calibration method is to use the same heat transfer multiplier for both the refrigerant side and the water side; another is to assume a constant water side multiplier and then solve the variable refrigerant side multiplier.

It has to be mentioned, for the fluted tube-in-tube water-to-refrigerant heat exchangers, the refrigerant flows outside and the water flows inside. The insulation layer wrapping the water-to-refrigerant heat exchanger was not perfect, and there could be a noticeable amount of heat exchanged with the environment. Our model can't account for this effect, due to unknown surrounding conditions. Another factor is that we don't know the exact tube inside and outside surface area due to the fluted shape. The model was based on typical tube geometry, not the same as the actual configuration. Thus, we have to depend on the calibrations and the heat transfer multipliers to include these factors. And the multipliers can be larger than 1, because of the extra heat transfer and the fluted surfaces.

We assumed that the correct water-side heat transfer multiplier should lead to minimum variation in the corresponding refrigerant heat transfer adjustments over the range of operating conditions. This is because the water-side correlations in Rousseau (2003) are more fully developed for a range of conditions and geometries than those for the refrigerant-side. We did a parametric study by varying the water side multiplier input. Then, we used the GenOpt® wrapper to solve the

refrigerant side heat transfer multipliers for the total forty points, referenced to each water side multiplier. Figures 5 and 6 show variability of the refrigerant side heat transfer multipliers (forty points) changing with the water side heat transfer multipliers, respectively for the condenser and evaporator. In these figures, we calculated the indicator for the variability of the heat transfer multiplier as the standard deviation of the forty-point population divided by the average refrigerant side heat transfer multiplier, at each water side heat transfer multiplier. For the condenser calibration, we varied the water side heat transfer multiplier from 1.0 to 2.5, with step of 0.5. As illustrated in Figure 5, the water side multiplier of 1.5 leads to minimum variation in the refrigerant side multipliers. For the evaporator side, we varied the water side multiplier from 1.0 to 3.0 with step of 0.5, and the water side multiplier of 2.5 leads to minimum variation in the refrigerant side multipliers. Thus, the constant water side multiplier of 1.5 for the condenser, 2.5 for the evaporator, and the corresponding set of refrigerant side heat transfer multipliers were adopted. Figures 7 and 8 show the condenser refrigerant side heat transfer multipliers, changing with the compressor speed, EWT and EHWT. We believe that the size of the multipliers may be related to unaccounted heat loss effects to/from the heat exchangers to ambient.

As observed in Figure 3, 4, 7 and 8, it is quite clear that the multipliers change with the operating conditions. Thermal system and component models are effective tools for engineering design and academic research. However, the mathematical models are just approximations of reality, trying to capture the most important factors. They can't consider all the factors, for example, oil influence, etc., and effects of these factors which change with operating conditions. If more data is available, functional calibration can further reduce the model inaccuracies in the range of operation conditions.

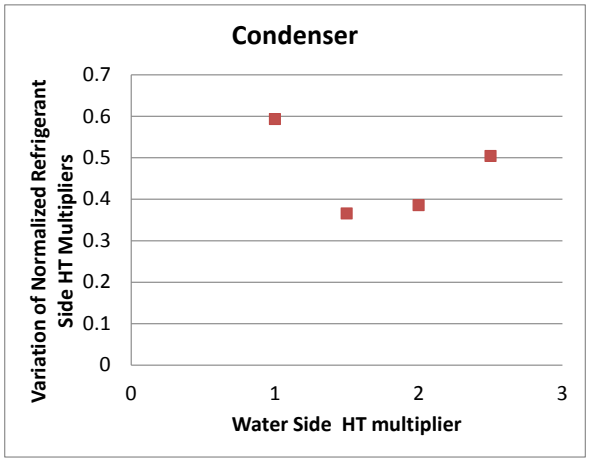

Figure 5: Variation of Condenser Refrigerant Side HT Multipliers Changing with Water Side HT Multiplier

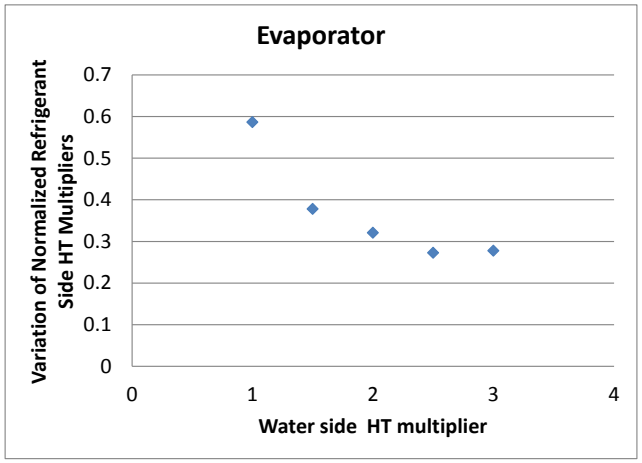

Figure 6: Variation of Evaporator Refrigerant Side HT Multipliers Changing with Water Side HT Multiplier

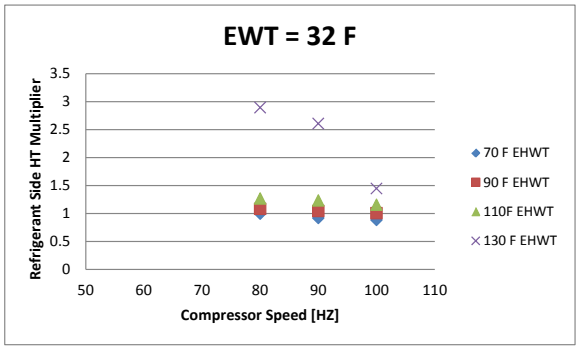

Figure 7: Condenser Refrigerant Side HT Multipliers Changing with EHWT and Compressor Speed at EWT = 0 °C, 32°F

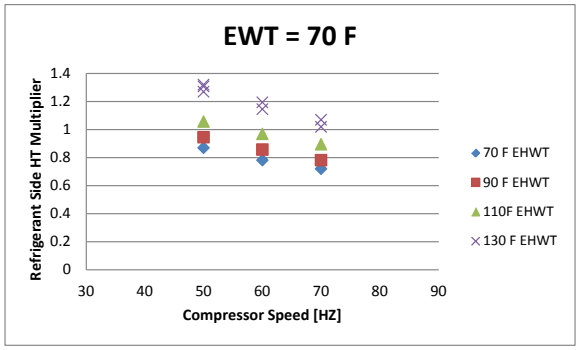

Figure 8: Condenser Refrigerant Side HT Multipliers Changing with EHWT and Compressor Speed at EWT=21.1 °C, 70°F

Based on the results of the forty-point calibration, we curve-fitted the PAFs, of compressor power consumption, ratio of compressor shell heat loss to compressor power, suction line heat gain, condenser and evaporator heat transfer and superheat degree, as a function of compressor speed, EWT and EHWT. And then, we incorporated the curves to improve the model prediction accuracy. The 3-dimensional calibration curves are fitted in the form of,

$$PAF = c_0 + c_1 \cdot HZ + c_2 \cdot EWT + c_3 \cdot EHWT + c_4 \cdot HZ^2 + c_5 \cdot EWT^2 + c_6 \cdot EHWT^2 + c_7 \cdot HZ \cdot EWT + c_8 \cdot HZ \cdot EHWT + c_9 \cdot EWT \cdot EHWT \quad (3)$$

Applying the 3-D calibration curves can effectively increase the model accuracy over the entire operating range. Figures 9 to 10 show comparisons between using the 3-D calibration curve and the average multiplier for the refrigerant heat transfer correction. These two figures are two-box plots, which compare distributions of two populations, i.e. the prediction deviations using a 3-D calibration curve or using an average heat transfer multiplier. A rectangular box for each group represents the middle 50% (interquartile range) of the data. The median value is indicated by the horizontal line inside the box. Lines extending from the box represent the upper and lower 25% of the distribution (excluding outliers). Outliers are indicated by asterisks beyond the whiskers. The average heat transfer multiplier was obtained from the forty cases. The 3-D curves reduce the scattering of the prediction errors for both the suction saturation temperature and the discharge saturation temperature. The deviations of the suction and discharge saturation temperatures are given in the form of predicted temperature minus measured temperature, for example, if the predicted saturation temperature is -0.56 °C (31 °F), and the measured saturation temperature is 0 °C (32 °F), the deviation is -0.56 °C (-1.0 °F).

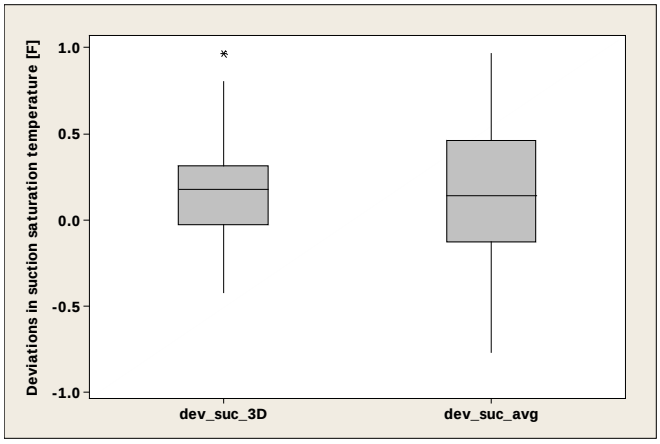

Figure 9: Distributions of Prediction Deviations for Predicting Suction Saturation Temperature, with Applying a 3-D Curve and an Average Multiplier

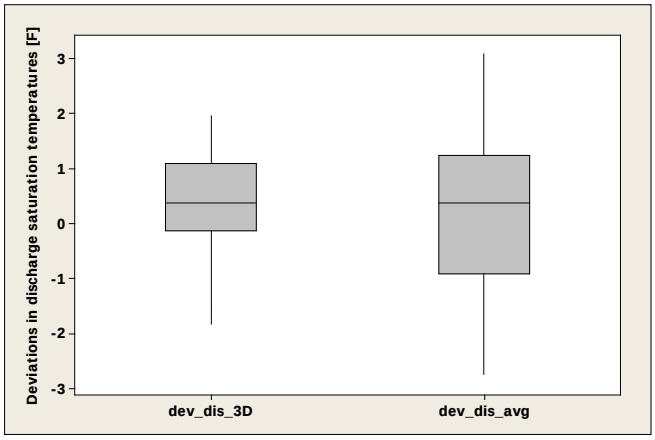

Figure 10: Distributions of Prediction Deviations for Predicting Discharge Saturation Temperature, with Applying a 3-D Curve and an Average Multiplier

CONTROL STRATEGY DETERMINATION

Available data showed that functional calibration improved the model accuracy over the operating range, which boosts the confidence in using the model to prescribe a control strategy over the entire operating envelope. The control strategy for an all variable-speed system is complicated, since it may have multiple adjustable variables and several objectives to pursue. High efficiency operation in the entire operating envelope is desirable for most products. However, the efficiency (COP, Coefficient of Performance) is not generally a measurable quantity during operation, and it needs to couple the behavior of all the components in the system. Consequently, the optimal control strategy, i.e. the relationship of the adjustable variables, has to be pre-defined. GenOpt® coupled with the system model provides a powerful tool for optimizing the equipment

performance over the entire operating envelope.

During the optimization of the ground source heat pump water heater, we kept the water delivery temperature around 57.2 °C (135°F), employing a once-through approach, to allow hot water to be supplied to the top of the tank while limiting the delivery temperature so as to not penalize the efficiency by over-heating. The compressor operation had constraints; these were to keep the suction saturation temperature below 15.6 °C (60 °F) (to provide sufficient cooling for the motor), and above -6.7 °C (20°F) (to prevent freezing the glycol in the ground loop). The available operating range for the variable-speed compressor was between 30 HZ to 120 HZ. Both the ground loop pump and water heater pump were capable of operating between 6.3e-5 m^3/s (1 GPM) and 6.3e-4 m^3/s (10 GPM). These constraints were used for maximizing system efficiencies over the entire operating range.

The optimization problem comprises three adjustable variables and three objectives. The adjustable variables are: compressor speed, varied from 30 HZ to 120 HZ; and the two pump flow rates varied from 6.3e-5 m^3/s (1 GPM) and 6.3e-4 m^3/s (10 GPM).The water delivery temperature is a target objective (equality constraint), which should match 57.2 °C (135°F), this target objective was assigned a weighting factor of 10.0. The compressor suction saturation temperature is a bound objective (inequality constraints), which has the upper bound of 15.6 °C (60°F) and lower bound of -6.7 °C (20°F), this bound objective was assigned a penalty factor of 1000. The penalty factors can be defined by the user, to rank the severities, for example, the penalty factor of 1000.0 indicates the condition should never happen, while the penalty factor of 1.0 indicates moderately acceptable. Finally, the COP is the optimization objective with a weight factor of -1, intended to maximize the value. We laid an optimization matrix for different operating conditions: the EWT ranged from 0 °C (32 °F) to 22.2 °C (72 °F), incremented by 2.8 K (5 °R), and EHWT ranged from 21.1 °C (70 °F) to 54.4 °C (130 °F), incremented by 2.8 K (5 °R). That means that we ran 117 GenOpt® cases in total to pursue optimal system performance over the entire operating domain. When running these cases, we specified a system charge to run the vapor compression system model; the charge was obtained as the average from the forty-point calibrations with specifying the measured condenser subcooling degrees.

Figures 11 to 14 show contour plots of the adjustment variables and the controlled objectives as a function of EWT and EHWT resulted from the GenOpt® optimization runs. We can see in Figure 11, that the water heater maintains the delivery water temperature around 57.2 °C (135 °F), except at the left bottom corner, where both the EHWT and EWT are low due to limitations of the compressor, and the two pumps. Figure 12 demonstrates the required ground loop flow rate. At low EHWT, the ground loop tends to flow at the largest flow rate of 6.3e-4 m^3/s (10 GPM), particularly with EWT lower than 10 °C (50 °F), because it needs to withdraw maximum heat from the source evaporator. The ground flow GPM decreases towards higher EHWT, and EWT, where lower ground flow rates lead to higher efficiency by reducing the pump power, while still maintaining the 57.2 °C (135°F) water delivery temperature. Figure 13 illustrates the required water heating GPM, which is mainly dependent on EHWT. The water heating GPM increases with increasing the EHWT towards 57.2 °C (135°F), considering at a fairly constant water heating capacity, smaller water temperature increase is coupled with larger water flow rate. At the EHWT of 21.1 °C (70°F), the water heating pump runs at the lowest flow rate around 6.3e-5 m^3/s (1 GPM). Figure 14 shows the required compressor speed contours. It is interesting to see that the compressor speed is around 95 HZ, instead of the largest speed, around the left bottom corner, for the case where the largest capacity is required to match the 57.2 °C (135°F) water delivery temperature. The reason for this is that the suction saturation temperature starts hitting the lower bound of -6.7 °C (20°F). In the temperature range where is no risk of freezing, the compressor speed reaches two peaks around 110 HZ, in order to match the 57.2 °C (135°F) water delivery temperature. Next, the compressor speed gradually decreases with increasing the EWT and EHWT, thereby unloading the heat exchangers to achieve better efficiency.

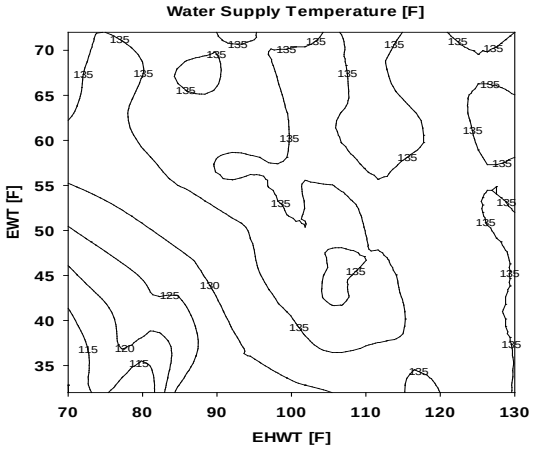

Figure 11: Heat Pump Water Delivery Temperature Contour

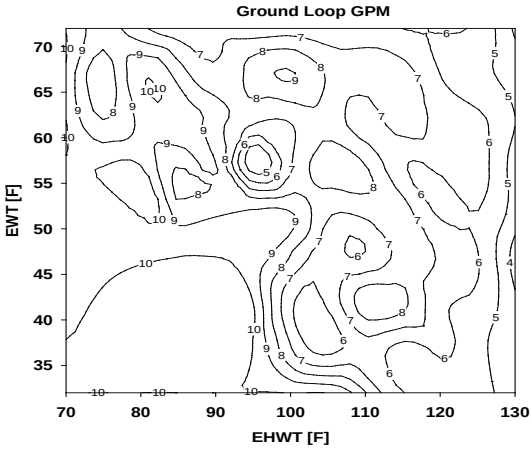

Figure 12: Ground Loop Flow Rate Contour

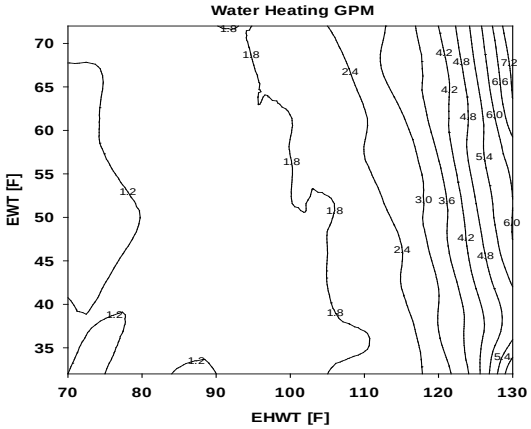

Figure 13: Water Heating GPM Contour

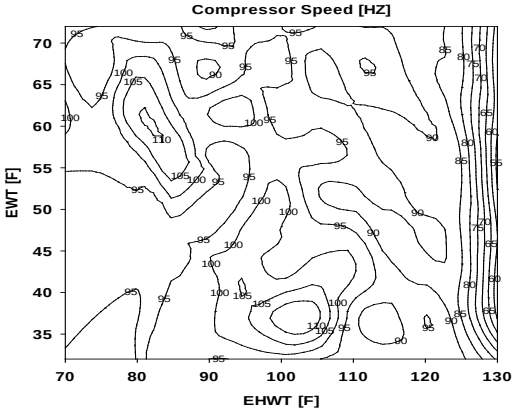

Figure 14: Compressor Speed Contour

The GenOpt® optimizer allows us to easily switch a control scenario. Based on the control strategy discussed earlier, we added an additional control objective: to achieve largest water heating capacity (faster water heating response). In this case, the water heating capacity is added as an optimum objective, having a weight factor of -1. Certainly, better efficiency and larger capacity are conflicting goals in some conditions. The GenOpt® optimizer only evaluates the output function described in Equation (2). The given weight factors impact the trade-off. It is noted that the COP and the water heating capacity were normalized during this optimization study.

Figures 15 and 16 show the impact of considering the water heating capacity during the optimization on system COP and capacity. The deviations are given as the deviation between the value when considering the capacity and the original optimization problem, divided by the value of the original optimization problem. It can be seen that there are no efficiency and capacity differences at small EWTs and EHWTs, where the equipment was running near the largest capacity to meet the delivery temperature constraint at a reasonable efficiency. At higher EWTs and EHWTs, there are regions to alter the compressor speed and pump flow rates, the strategy with maximizing the capacity increases the capacity up to 80%, but at the expense of reducing the efficiency by 15%. Certainly, the conclusion will be different if we apply different weight factors for efficiency and capacity. Engineers can decide the most reasonable trade-off for the final design.

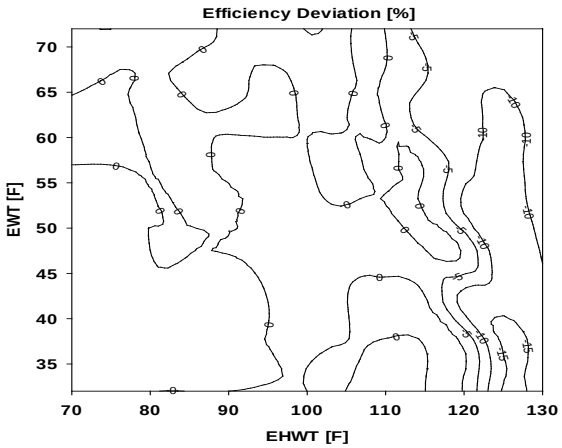

Figure 15: Contour of Efficiency Deviations with/without Optimizing the Water Heating Capacity

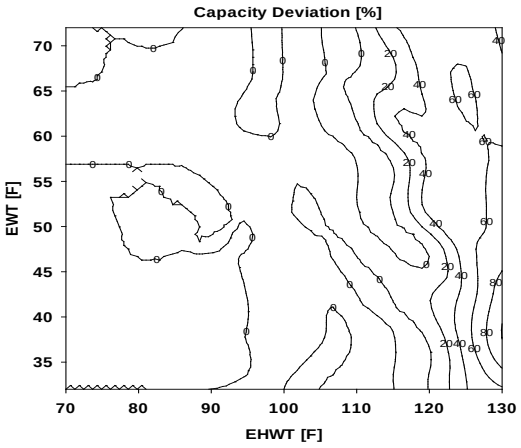

Figure 16: Contour of Capacity Deviations with/without Optimizing the Water Heating Capacity

CONCLUSIONS

The GenOpt® wrapper program accepts objectives for optimizing, targeting, and bounding. It can be a flexible and powerful tool for model calibration, control strategy determination, and product configuration optimization. Also, it considers design constraints by setting bounding objectives. Furthermore, it enables parametric optimization runs in an extensive range, and helps engineers to achieve optimized design over an entire operation envelope.

Manual calibration can be a time-consuming and error-prone practice. The GenOpt® wrapper provides an auto-calibration means by selecting targeting objectives. The auto-calibration function makes it possible for engineers to calibrate a system model against experimental data over a large range. Based on these, engineers can apply functional calibration curves to improve the model accuracy for extensive operation conditions.

Variable-speed products bring in multiple adjustable variables and control objectives. Engineering rules of thumb and trial-and-error approach don't work anymore for such a high level of complexity. An effective optimization tool is indispensible for designing high efficiency equipment. This paper describes an approach for developing an optimized control strategy for a once-through all variable-speed, ground source, heat pump water heater. This main purpose of this study is to demonstrate of the optimization package's capabilities, while the investigated control strategy is not necessarily the most efficient approach, according to various application scenarios.

REFERENCES

AHRI, 2004. Standard For Performance Rating Of Positive Displacement Refrigerant Compressors And Compressor Units, Air-Conditioning, Heating, and Refrigeration Institute, Arlington, VA

Hooke R. and Jeeves. T. A., "Direct search solution of numerical and statistical problems". Journal of the Association for Computing Machinery, 8(2):212–229, 1961.

Kennedy J. and Eberhart. R. C. "Particle swarm optimization." In IEEE International Conference on Neural Networks, volume IV, pages 1942–1948, Perth, Australia, November 1995.

Kennedy J. and Eberhart. R. C. "A discrete binary version of the particle swarm algorithm." In Proc. of Systems, Man, and Cyber-netics, volume 5, pages 4104–4108. IEEE, October 1997.

Nelder J. A. and Mead. R., "A simplex method for function mini-mization." The computer journal, 7(4):308–313, January 1965.

Rousseau P.G., M. van Eldik, G.P. Greyvenstein, “Detailed simulation of fluted tube water heating condensers”, International Journal of Refrigeration 26 (2003) 232–239.

Rice, C. K.and W.L.Jackson, 2005. DOE/ORNL Heat Pump Design Model, Mark VI, http://www.ornl.gov/~wlj/hpdm/MarkVI.shtml

Rossi, T.M. 1995 “Detection, diagnosis, and evaluation of faults in vapor compression cycle equipment.” Ph.D. thesis, Herrick labs, Purdue University, Ind. Report No. 1796-3 HL 95-13

Radermacher, Reinhard; Abdelaziz, Omar Source: HVAC and R Research, v 14, n 6, p 817-818, November 2008. "Optimization" and HVAC&R

Wetter, M., “GenOpt® Generic Optimization Program User Manual Version 3.0.0”, May 11, 2009, Lawrence Berkeley National Laboratory Technical Report LBNL-2077E